

Supplementary Materials

Selective *a*-domain switching by sub-coercive field in PbTiO₃ thin films

Kil-dong Sung^{1,#}, Min-Su Kim^{2,#}, Jinhyuk Jang², Gi-Yeop Kim², Kyung Song³, Si-Young Choi^{2,4}, Seungbum Hong⁵

¹Institute of Physics of the Czech Academy of Sciences (FZU), Prague 182 00, Czech Republic.

²Department of Materials Science and Engineering, Pohang University of Science and Technology (POSTECH), Pohang 37673, Republic of Korea.

³Department of Materials Analysis and Evaluation, Korea Institute of Materials Science (KIMS), Changwon 51508, Republic of Korea.

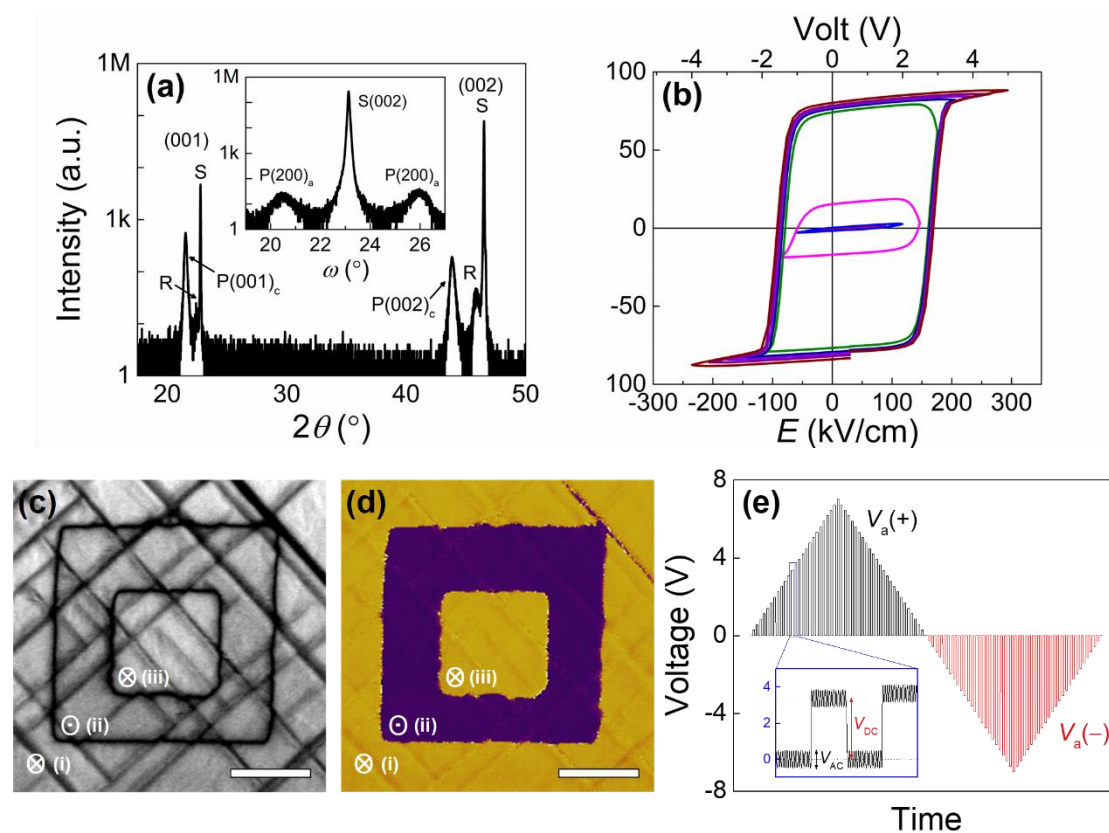
⁴Department of Semiconductor Engineering, Pohang University of Science and Technology (POSTECH), Pohang 37673, Republic of Korea.

⁵Department of Materials Science and Engineering, Korea Advanced Institute of Science and Technology (KAIST), Daejeon 34141, Republic of Korea.

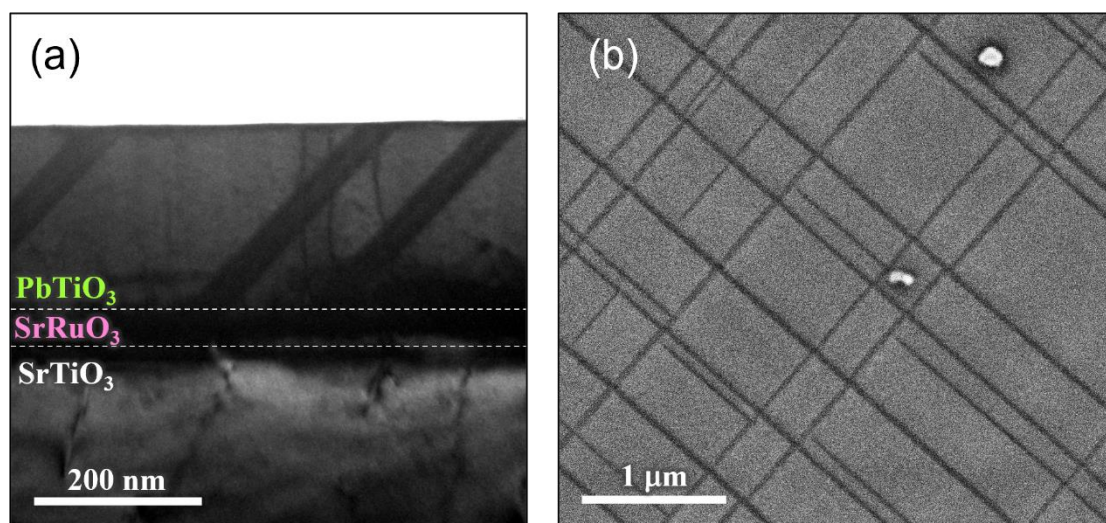
These authors contributed equally to this work.

Correspondence to: Dr. Kil-dong Sung, Institute of Physics of the Czech Academy of Sciences (FZU), Prague 182 00, Czech Republic. E-mail: sung@fzu.cz; Prof./Dr. Si-Young Choi, Department of Materials Science and Engineering, Pohang University of Science and Technology (POSTECH), Pohang 37673, Republic of Korea; Department of Semiconductor Engineering, Pohang University of Science and Technology (POSTECH), Pohang 37673, Republic of Korea. E-mail: youngchoi@postech.ac.kr

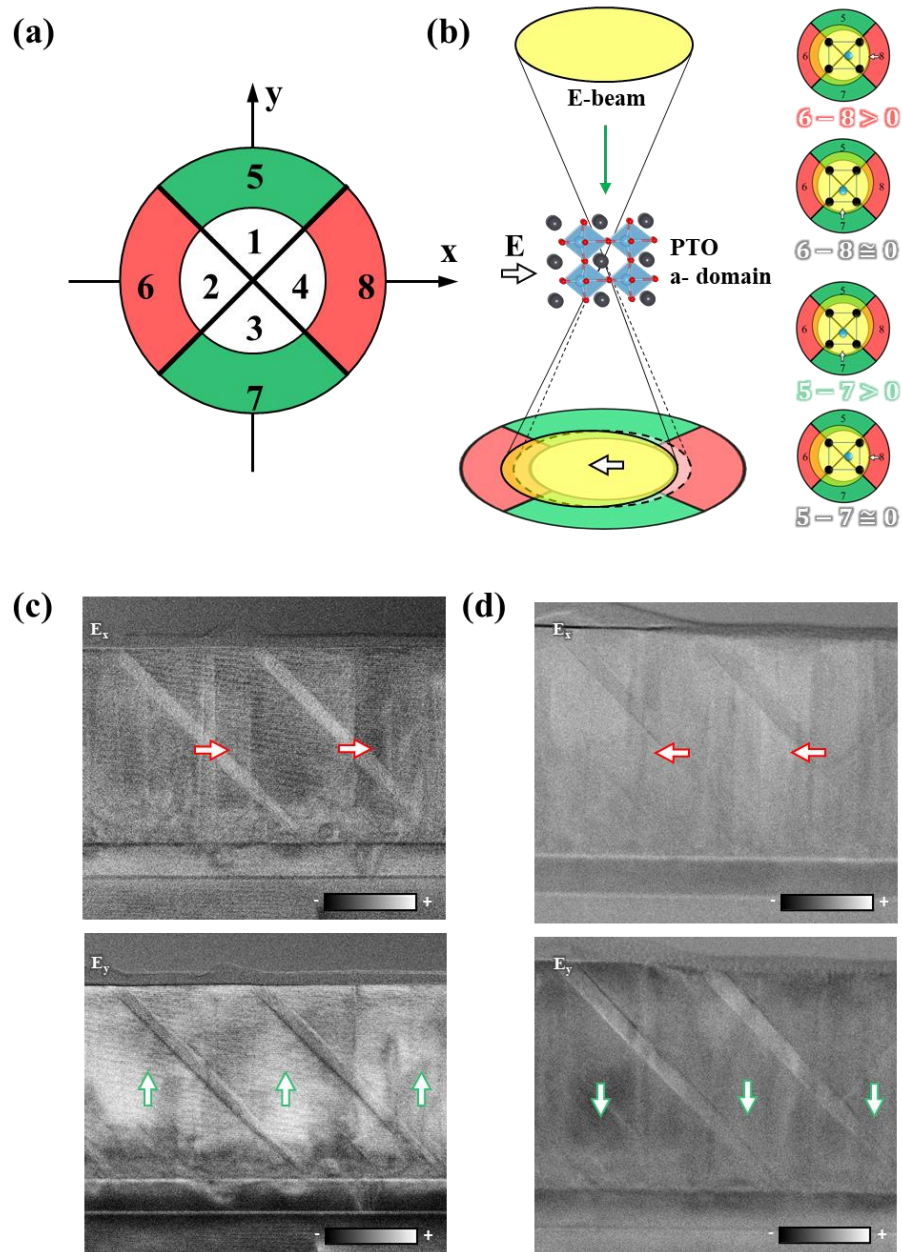
ORCID: Kil-dong Sung (0000-0003-2803-9292), Si-Young Choi (0000-0003-1648-142X)



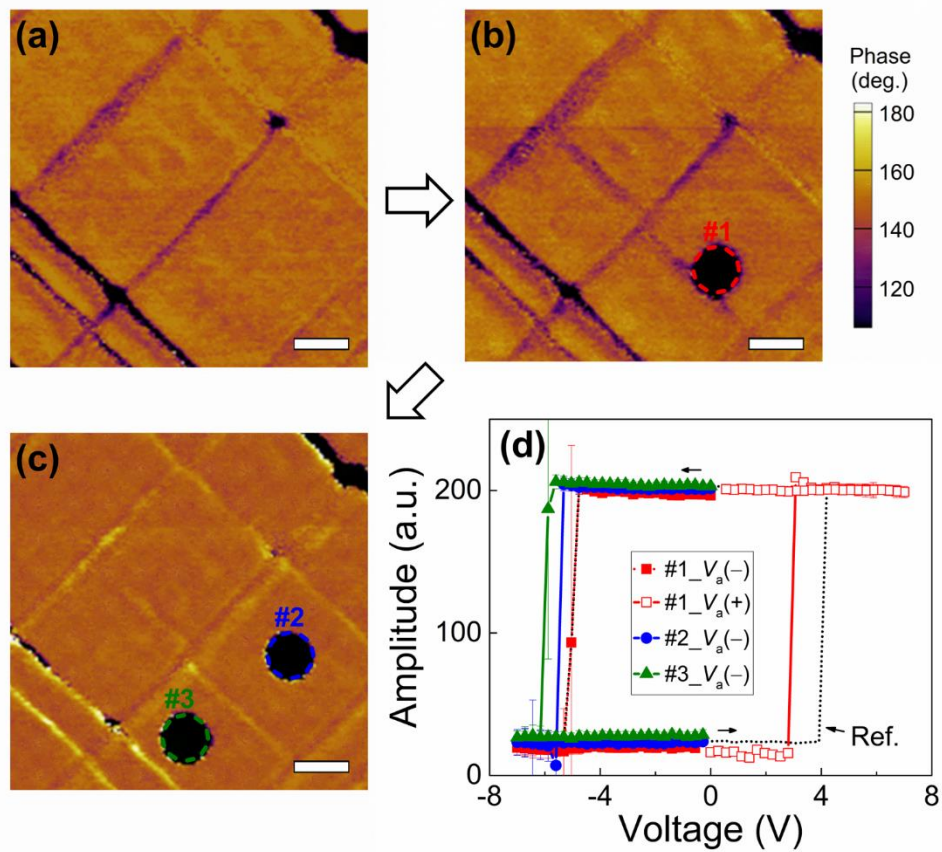
Supplementary Figure 1. (a) HR-XRD θ - 2θ pattern of PTO (P)/SRO (R)/STO (S) thin films. The rocking curve shown in the inset reveals the presence of the a -domain in the PTO layer, indicated by $P(200)_a$ peaks, while the c -domain is represented by $P(002)_c$ peak in the θ - 2θ scan. (b) Electric polarization-electric field (P - E) (P - E) curves at 1 kHz for various maximum electric fields. The upper x -axis indicates the corresponding voltage. PFM (c) amplitude and (d) phase images of (i) $V_{DC} = 0$ V, (ii) $V_{DC} = -7$ V, and (iii) $V_{DC} = +7$ V tip-biased regions, with upward and downward electric polarization. The scale bar represents 500 nm. (e) Voltage bias sweep sequences with DC and AC voltages. $V_a(+)$ (black line) and $V_a(-)$ (red line) indicate positive and negative DC voltage biases, respectively.



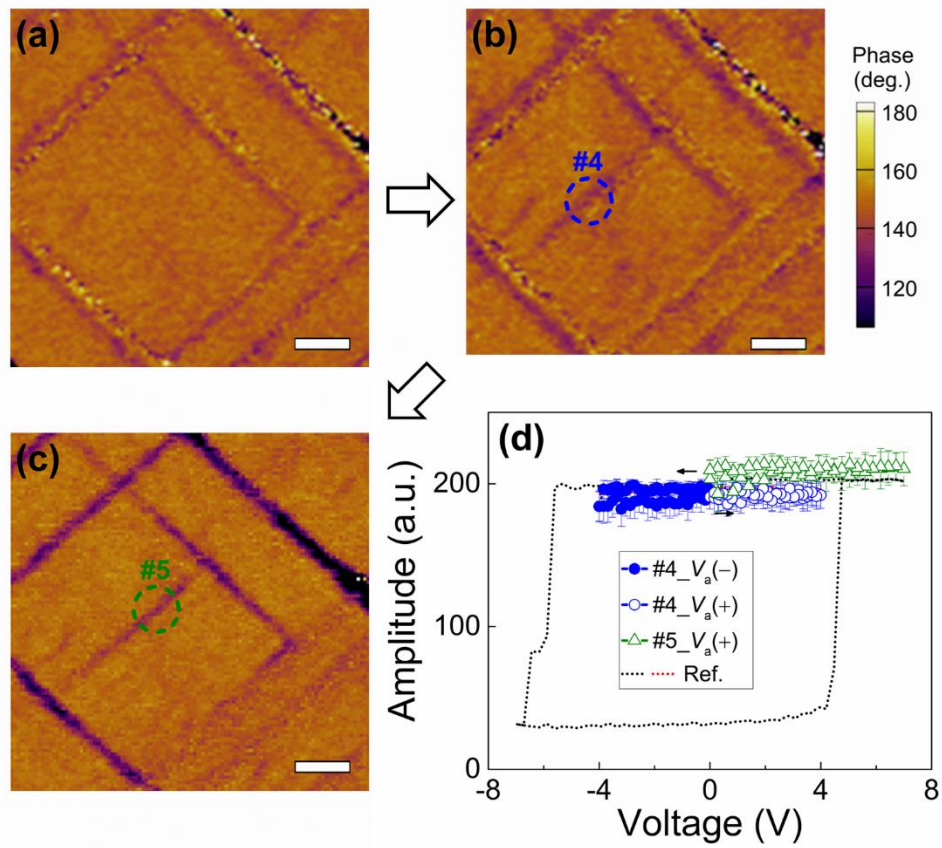
Supplementary Figure 2. (a) Cross-sectional BF-TEM image for the PTO/SRO/STO heterostructures. (b) SEM image representing the surface topography of PTO film. The dark and gray contrast in PTO film represents a -domain and c -domain, respectively for both images.



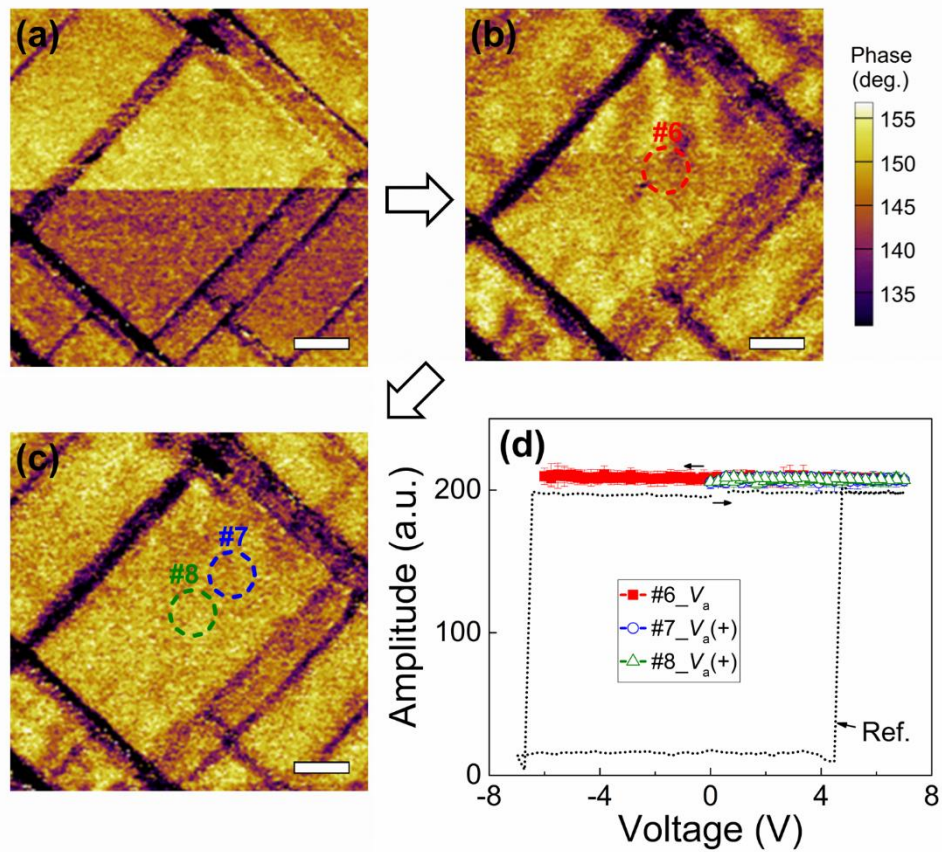
Supplementary Figure 3. (a) Schematic diagram of a segmented annular all-field detector for DPC imaging. Angular ranges of segments 1~4 and 5~8 are 0~24 mrad and 24~48 mrad, respectively. (b) Schematic diagram of the electron beam path deflected by the internal field of *a*-domain PTO. The deflected beam signals arrive at shifted positions from the center of the segmented detector. DPC images of electric fields with the components of the *x*-direction and *y*-direction segments for (c) before and (d) after poling. As the external electric field applied by corona poling drives the switching of polarization direction in both of *a*- and *c*-domain structures.



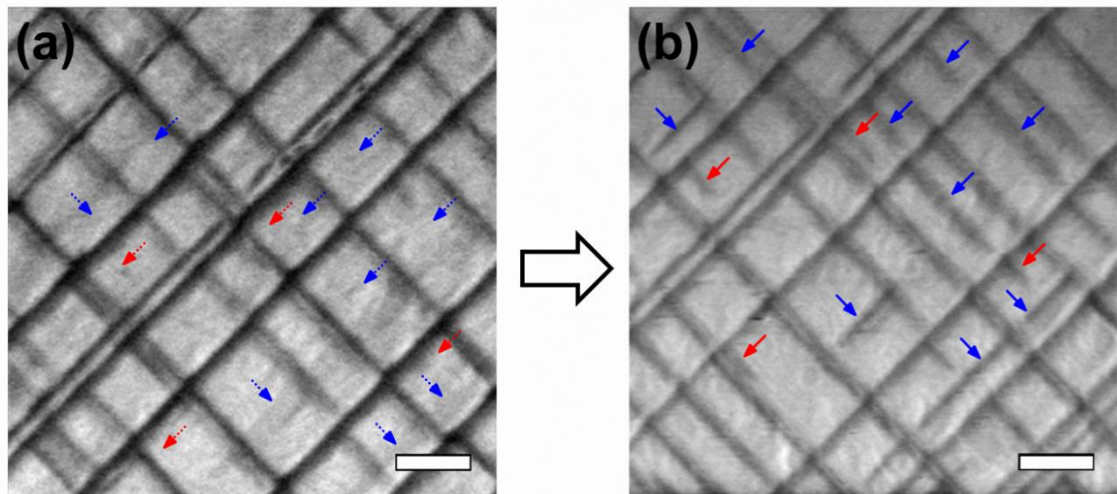
Supplementary Figure 4. PFM phase images of (a) the initial state, (b) $V_a = -7\text{V}$ at position #1, and (c) $V_a = -7\text{V}$ at positions #2 and #3 following $V_a = +7\text{V}$ at position #1. The white scale bar represents 200 nm. (d) Voltage-dependent PFM phase curves measured at positions #1 (red squares), #2 (blue circles), and #3 (green triangles) under negative ($V_a(-)$, closed symbols) and positive ($V_a(+)$, open symbols) bias. The conventional phase response near the tested c -domain (dotted black line) is shown for reference. Black arrows indicate the direction of the voltage sweeps.



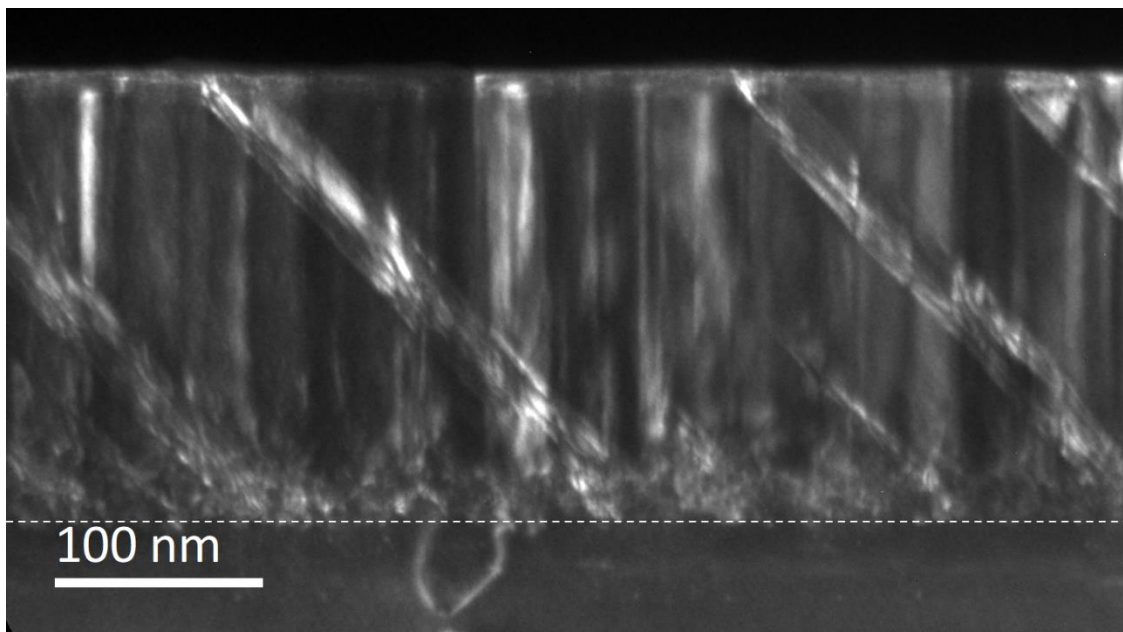
Supplementary Figure 5. PFM phase images of (a) the initial state, (b) $V_a = -4\text{V}$ at position #4, and (c) $V_a = +4\text{V}$ at positions #4 following $V_a = +7\text{V}$ at position #5. The white scale bar represents 200 nm. (d) Voltage-dependent PFM phase curves measured at positions #4 (blue circles), #5 (green triangles) under negative ($V_a(-)$, closed symbols) and positive ($V_a(+)$, open symbols) bias. The conventional phase response near the tested c -domain (dotted black and red lines) is shown for reference. Black arrows indicate the direction of the voltage sweeps.



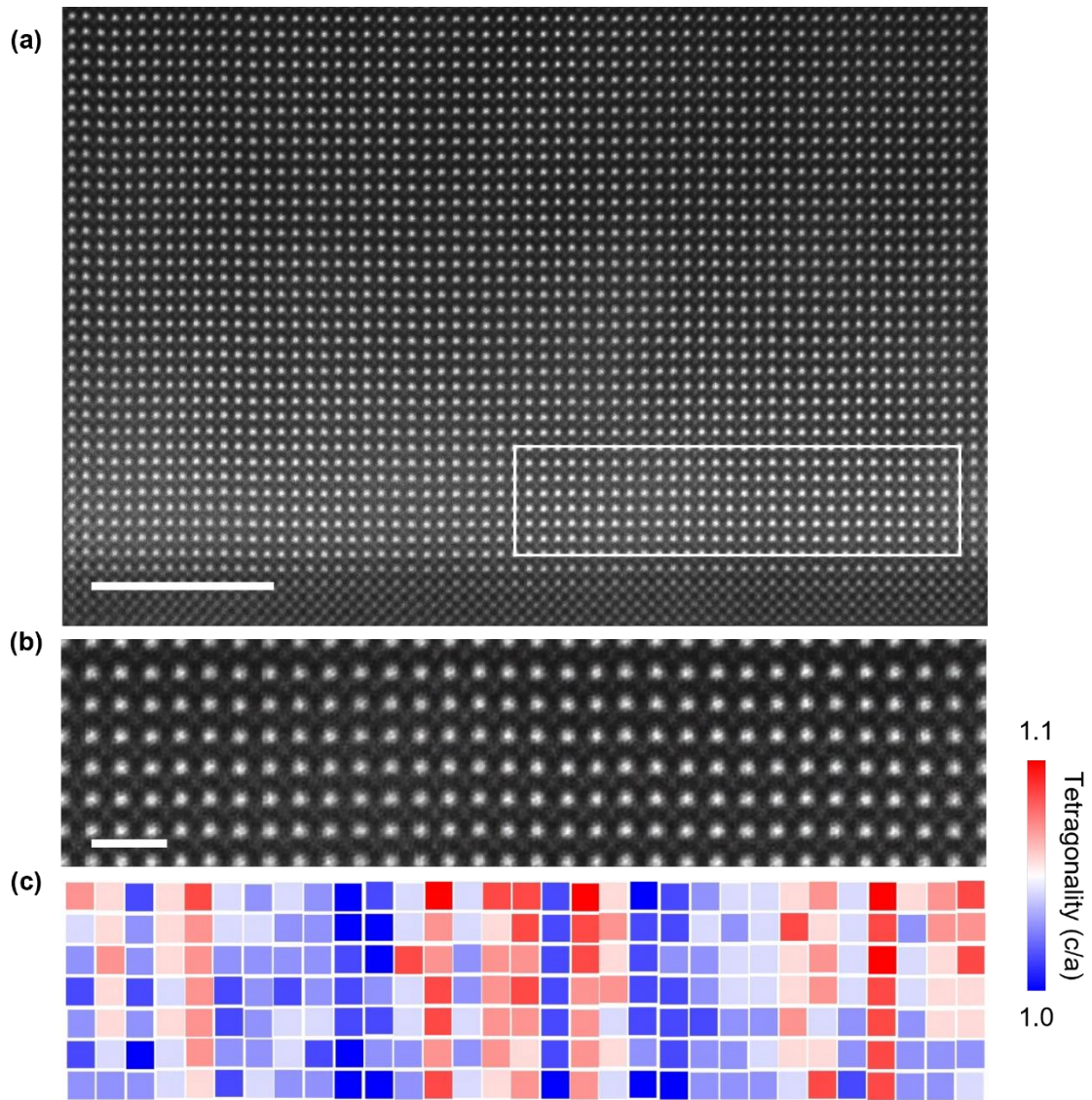
Supplementary Figure 6. PFM phase images of (a) the initial state, (b) $V_a = -4\text{V}$ followed by $+4\text{V}$ at position #6, and (c) $V_a = +7\text{V}$ at positions #7 and #8. The white scale bar represents 200 nm. (d) Voltage-dependent PFM phase curves measured at positions #6 (red squares), #7 (blue circles), and #8 (green triangles) under bipolar (V_a , closed symbols) and positive ($V_a(+)$, open symbols) bias. The conventional phase response near the tested c -domain (dotted black lines) is shown for reference. Black arrows indicate the direction of the voltage sweeps.



Supplementary Figure 7. PFM amplitude images of the sample (a) before and (b) after *a*-domain formation upon the area bias application at $V_{CD} = -4$ V. Blue and red arrows indicate the fully and partially connected *a*-domains, which represent the irreversible and reversible *c*- to *a*-domain switching, respectively. The white scale bar represents 400 nm.



Supplementary Figure 8. DF-TEM image observed along the cross-sectional view for the PTO/SRO/STO heterostructure. The threading dislocation and interfacial strain appears abnormal contrast in the PTO film. White dotted lines represent the interface between PTO/SRO.



Supplementary Figure 9. (a) Atomic-scale HAADF-STEM image of PTO/SRO. (b) Cropped HAADF-STEM image indicated by white box in (a). (c) Calculated tetragonality of PTO lattice near the interface. Each unit cell is defined using atomic positions of four neighboring A-site ions, Sr, and the tetragonality (c/a) is calculated using the center of mass of the A-site atom column intensity. As the PTO is the tetragonal ferroelectrics, the range of tetragonality is from 1.0 to 1.1, and the remaining local strain is clearly observed with a higher c/a value. The scale bar is 5 nm in (a) and 1 nm in (b), respectively.

Theoretical Calculations

The free energy of PTO consisting of *a*- and *c*-domains can be calculated by considering both electrostatic and elastic contributions. The electrostatic energy (ΔU_i^{es}) of each domain is given by

$$\begin{aligned}\Delta U_i^{es} &= U_i^{es}(E) - U_i^{es}(E = 0) \\ &= - \int_0^{\vec{E}} \vec{P}_i \cdot d\vec{E} \approx -\vec{P}_i \cdot \vec{E}\end{aligned}$$

where, \vec{P}_i is the electric polarization, *i* denotes the *a*- or *c*-domain, and \vec{E} is the applied electric field. Therefore $\vec{P}_a \cdot \vec{E} \approx 0$ and $\vec{P}_c \cdot \vec{E} = -P_c V/d$, where *V* is the applied voltage and *d* is the thickness of PTO film.

The elastic energy (ΔU^{el}) depends on both external voltage (*V*) and the substrate-film misfit (Φ). Consequently, both the voltage-induced elastic energy of individual domains, $\Delta U_i^{el}(V)$, and the misfit-induced elastic energy of the *a/c*-domain combination, $\Delta U_w^{el}(\Phi)$, should be considered. For individual domains, $\Delta U_i^{el}(V)$ can be expressed as

$$\begin{aligned}\Delta U_i^{el}(V) &= \frac{Y}{2(1+\nu)(1-2\nu)} [(1-\nu)(\varepsilon_{11,i}^2 + \varepsilon_{22,i}^2 + \varepsilon_{33,i}^2) + 2\nu(\varepsilon_{11,i}\varepsilon_{22,i} + \varepsilon_{22,i}\varepsilon_{33,i} + \varepsilon_{11,i}\varepsilon_{33,i})] \\ &\quad + \frac{Y}{4(1+\nu)} (\varepsilon_{12,i}^2 + \varepsilon_{23,i}^2 + \varepsilon_{13,i}^2)\end{aligned}$$

where, *Y* is Young's modulus, ν is Poisson's ratio, and $\varepsilon_{jk,i}$ is the strain tensor of the *a/c*-domain. The voltage-induced strain is $\varepsilon_{jk,i} = d_{jk,i}E$, where $d_{jk,i}$ is the piezoelectric coefficient tensor. Accordingly,

$$\begin{aligned}\Delta U_c^{el}(V) &= \frac{Y(2d_{31}^2 + (1-\nu)d_{33}^2 + 4\nu d_{31}d_{33})V^2}{2(1+\nu)(1-2\nu)d^2} \\ \Delta U_a^{el}(V) &= \frac{Yd_{24}^2}{4(1+\nu)} \frac{V^2}{d^2}\end{aligned}$$

with

$$\begin{aligned}\varepsilon_{11,c} &= d_{31} \frac{V}{d}; \varepsilon_{22,c} = d_{31} \frac{V}{d}; \varepsilon_{33,c} = d_{33} \frac{V}{d}; \varepsilon_{12,c} = \varepsilon_{23,c} = \varepsilon_{13,c} = 0 \\ \varepsilon_{11,a} &= \varepsilon_{22,a} = \varepsilon_{33,a} = \varepsilon_{12,a} = \varepsilon_{23,a} = 0; \varepsilon_{13,a} = d_{24} \frac{V}{d}\end{aligned}$$

Unlike $\Delta U_i^{el}(V)$, which considers *a*- and *c*-domains individually, $\Delta U_w^{el}(\Phi)$ accounts for the elastic interaction between domains. Assuming constant Φ over the layer, the local in-plane strain (ε_a) is treated as an independent variable to determine $\Phi(\varepsilon_a)$ and $\alpha(\varepsilon_a)$, thereby understanding localized elastic energy variations during *a*- to *c*-domain switching. Accordingly, the elastic free energy associated with the formation of an *a*-domain within a *c*-domain matrix is

$$\Delta F_w(\varepsilon_a) = \Delta U_w^{el}(\varepsilon_a) + U_w$$

$$= \frac{Yd\alpha(\varepsilon_a)^2 \left(-2\pi\Phi(\varepsilon_a)(1+\nu)\xi + 2\xi \tan^{-1}\left(\frac{\xi}{2}\right) + \frac{1}{8}\xi^2 \log\left(1 + \frac{4}{\xi^2}\right) - 2 \log\left(1 + \frac{\xi^2}{4}\right) \right)}{2\pi(1-\nu^2)w_a} + \frac{2\sqrt{2}\lambda}{w_a}$$

Where

$$\alpha = \frac{c'_{\text{PTO}} - a'_{\text{PTO}}}{a'_{\text{PTO}}}, \quad \Phi = \frac{b_{\text{SRO}} - a'_{\text{PTO}}}{c'_{\text{PTO}} - a'_{\text{PTO}}}, \quad \xi = \frac{w}{d}, \quad \varepsilon_c = -\frac{2\nu}{1-\nu} \varepsilon_a,$$

$$a'_{\text{PTO}} = a_{\text{PTO}}(1 + \varepsilon_a), \quad c'_{\text{PTO}} = c_{\text{PTO}}(1 + \varepsilon_c),$$

with a_{PTO} and c_{PTO} being the lattice parameters of PTO, b_{SRO} the lattice parameter of SRO, w the a -domain width, w_a the averaged a -domain width from DPC, and λ the a/c -domain wall surface energy. The material parameters used are: $P_c = -80 \mu\text{C}/\text{cm}^2$, $d = 200 \text{ nm}$, $Y = 148 \text{ GPa}$, $\nu = 0.3$, $d_{31} = -23 \text{ pm/V}$, $d_{33} = 79 \text{ pm/V}$, $d_{24} = 56 \text{ pm/V}$, $a_{\text{PTO}} = 3.904 \text{ \AA}$, $c_{\text{PTO}} = 4.152 \text{ \AA}$, $b_{\text{SRO}} = 3.925 \text{ \AA}$, and $w_a = 20 \text{ nm}$. Consequentially, the total free energy of PTO during domain switching is obtained by summing up the electrostatic and elastic contributions:

$$\Delta F_{\text{total}} = \Delta F_c(V) + \Delta F_a(V) + \Delta F_w(\varepsilon_a).$$